

and J. R. DeKock, *Plasma Phys.* **23**, 903 (1981).

⁴F. S. Mozer *et al.*, *Phys. Rev. Lett.* **38**, 292 (1977);
F. S. Mozer *et al.*, *Space Sci. Rev.* **27**, 155 (1980).

⁵F. S. Mozer *et al.*, *J. Geophys. Res.* **84**, 5875 (1979).

⁶P. F. Mizera and J. F. Fennel, *Geophys. Res. Lett.* **4**, 311 (1977); E. G. Shelley, R. D. Sharp, and R. G. Johnson, *Geophys. Res. Lett.* **3**, 654 (1976); R. D. Sharp, R. G. Johnson, and E. G. Shelley, *J. Geophys. Res.* **82**, 3324 (1977).

⁷R. D. Croley, Jr., P. F. Mizera, and J. F. Fennel, *J. Geophys. Res.* **83**, 2761 (1978).

⁸P. M. Kintner *et al.*, *J. Geophys. Res.* **84**, 7201 (1979). See also M. A. Temerin, M. Woldorff, and F. S. Mozer, *Phys. Rev. Lett.* **43**, 1941 (1979); P. M. Kintner, *Geophys. Res. Lett.* **7**, 585 (1980), for other examples of ion-associated waves on auroral field lines. Space limitations prevent discussion of other solitary waves not associated with double layers seen in conjunction with steepened electrostatic ion-cyclotron waves.

⁹L. A. Frank and K. L. Ackerson, *J. Geophys. Res.* **76**, 3612 (1971).

¹⁰The uncertainty in the velocity estimate is due in part to the different gains and telemetry noise levels associated with the two double probes, which make it difficult to key on similar features in the data.

¹¹E. W. Laedke and K. W. Spatschek, *Phys. Rev. Lett.* **47**, 719 (1981).

¹²A. Hasagawa and T. Sato, *Bull. Am. Phys. Soc.* **25**, 844 (1980).

¹³W. Lotko, Ph.D. thesis, University of California, Los Angeles, 1981 (unpublished).

¹⁴D. A. Gurnett and R. R. Anderson, in *Physics of Auroral Arc Formation*, edited by S. I. Akasofu and J. R. Kan (American Geophysical Union, Washington, D.C., 1981), p. 341. Also see J. L. Green, D. A. Gurnett, and R. A. Hoffman, *J. Geophys. Res.* **84**, 5211 (1979); W. Calvert, *Geophys. Res. Lett.* **8**, 919 (1981), for other relevant features of auroral kilometeric radiation.

Stimulated Raman Scattering from uv-Laser-Produced Plasmas

K. Tanaka, L. M. Goldman,^(a) W. Seka, M. C. Richardson, J. M. Soures, and E. A. Williams
Laboratory for Laser Energetics, University of Rochester, Rochester, New York 14627
(Received 14 December 1981)

Time-integrated, spectrally resolved measurements between 400 and 750 nm have been made of light backscattered from plasmas produced by 450-psec pulses from a 351-nm laser at 10^{13} to 10^{15} W/cm². Threshold and saturation behavior for the two-plasmon decay and the absolute and convective Raman instabilities have been observed. The scattered light spectra suggest the presence of a steepened density profile at the quarter critical density.

PACS numbers: 52.25.Ps, 52.35.-g, 52.50.Jm, 52.70.Kz

Parametric processes in laser-produced plasmas can be sources of energetic electrons which, through their long mean free paths, may preheat the target core in laser fusion experiments and thus influence the hydrodynamics significantly.¹ Among the parametric processes, stimulated Raman scattering (SRS) and the two-plasmon ($2\omega_p$) decay instability may be efficient generators of hot electrons,² especially in the extensive underdense plasmas expected for inertial-confinement fusion targets. Observations of SRS from plasmas produced by 1064- and 532-nm lasers have recently been reported in the literature.³ The existence of the $2\omega_p$ instability has variously been inferred from $\frac{3}{2}\omega_0$ measurements⁴ and from direct plasma wave observations in CO₂-laser-produced plasmas by Baldis, Samson, and Corkum.⁵

In this Letter, we report backscattering measurements from plasmas produced by 351-nm

laser light which demonstrate (as a function of intensity) clear thresholds and low-level saturation for the $2\omega_p$ instability as well as for the absolute (SRS-A) and convective (SRS-C) Raman instabilities. Broad continuum spectra between 400 and 700 nm were observed for the SRS-C instability. The relatively small frequency change ($\Delta\omega$) associated with the low-wavelength limit of these spectra indicates that SRS is operative in plasma densities as low as $0.05n_c$ (n_c is the critical density for 351-nm radiation). The measurements do show the expected lower threshold for the $2\omega_p$ instability relative to the SRS-A instability as predicted by theory. However, the SRS-C is found to have approximately the same threshold as the SRS-A instability, instead of the considerably higher threshold expected if both instabilities operate in plasmas with comparable scale lengths.

The experiments described here were performed

on the single-beam uv irradiation facility at the Laboratory for Laser Energetics.⁶ An $f/12$ quartz lens was used to focus the linearly polarized light ($\lambda_0 = 351$ nm) on the target. Intensities between 10^{13} and 2×10^{15} W/cm² were obtained by varying both energy (10 to 50 J) and focal spot size (100 to 500 μ m) of the 450-psec pulses. The residual fundamental (1054 nm) and second-harmonic (527 nm) light from the frequency conversion typically account for $\lesssim 10^{-5}$ of the intensity at the target plane. Parylene (CH) slab targets, mostly oriented normal to the laser beam, were used throughout these experiments. A 0.25-m low-dispersion grating spectrograph with 1-nm resolution was used to resolve the light backscattered through the focusing optics between 400 and 750 nm. In addition, six calibrated photodiodes with interference filters were used for absolute measurements of the scattered light around 700 nm. The diodes were located around the target in the plane perpendicular to the plane of polarization of the incident beam.

The spectral dependence of the backscattered radiation between 400 and 750 nm is shown in Fig. 1. Curve *a* shows the scattered spectrum from a CH target irradiated at 4.6×10^{14} W/cm² ($\approx 10\%$ above the SRS threshold). We observe clear $\omega_0/2$ signals at 703 nm (SRS-A) as well as between 490 and 550 nm (SRS-C, $\Delta\omega < \omega_0/2$). Curve *b* illustrates the results well above threshold. The convective signal now ranges between 450 and 610 nm. The observation of noticeable

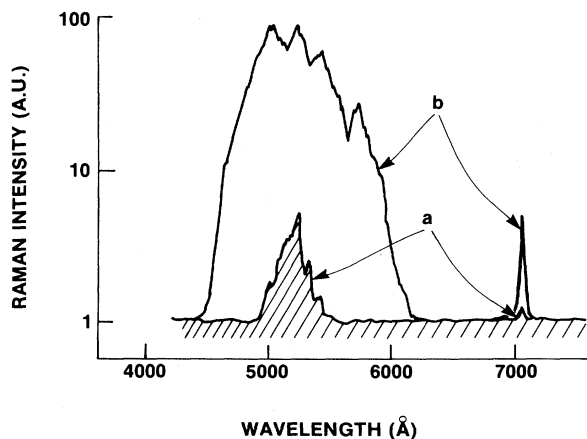


FIG. 1. SRS-A instability spectra from CH targets. Curve *a*, $I_{\text{inc}} = 1.1 \times I_{\text{SRS-A}}$; curve *b*, $I_{\text{inc}} = 3 \times I_{\text{SRS-A}}$, where $I_{\text{SRS-A}}$ is the SRS-A threshold intensity. The spectra have been recorded on Kodak high-speed ir film. The curves shown have been corrected for film response.

scattering at 450 nm ($\Delta\omega/\omega_0 \approx 0.2$) indicates that the SRS-C instability occurs at densities as low as $0.05n_c$.

Figure 2 shows plots of the intensity dependence of the fractional scattered light energy. The two upper curves were obtained with the absolutely calibrated photodiodes at 700 nm ($\omega_0/2$). Curve *a*, linking the solid points, represents measurements of the scattered light with polarization parallel to the incident laser polarization. Curve *b*, which links the open squares, represents observations with opposite polarization. Two separate sharp increases are evident in curve *a* at 4×10^{13} and 4×10^{14} W/cm². These are interpreted as the thresholds for the $2\omega_p$ and SRS-A instabilities, respectively. This interpretation is supported by the cross-polarized observations (curve *b*) which do not show the second rise. The polarization dependence of the scattering is explained by noting that for SRS one observes direct scattering events which remain highly polarized. In contrast, the $2\omega_p$ -instability light arises from

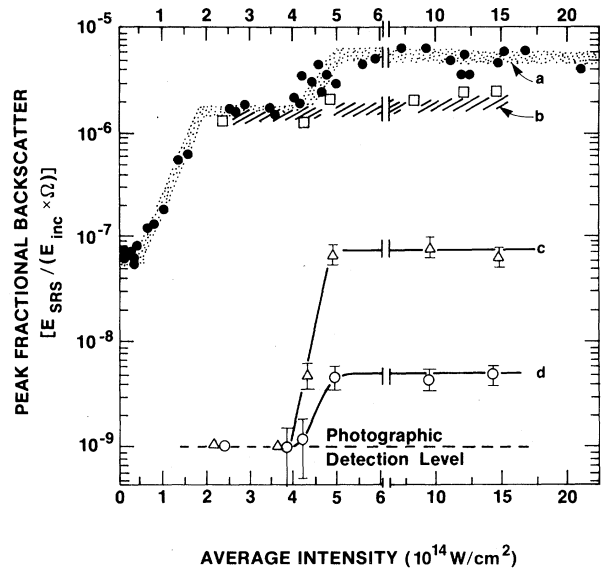


FIG. 2. Intensity dependence of SRS. Curves *a* and *b* are absolute backscattering measurements using calibrated photodiodes at 700 nm. The vertical axis represents the peak fluence in the angular distribution normalized to the incident energy in units of J/(J sr). Curve *a* is for scattered light polarized parallel to the incident laser; curve *b* is for opposite polarization. Curves *c* and *d* are similar curves obtained from spectrographic recordings at 700 and 500 nm. The vertical axis for these two curves is not absolutely calibrated. Curves *c* and *d* correspond to backscattering from the convective and absolute Raman instabilities, respectively.

a two-stage process, in which the original photon decays into two plasmons, each of frequency very near $\omega_0/2$, which may then reconvert into photons with frequency $\omega_0/2$. Possible reemission processes include direct conversion (the inverse process of resonance absorption) and various three-wave scattering processes. All these processes require a scattering of the plasma waves before reemission in order to produce the essentially unpolarized light shown in Fig. 2 below the Raman threshold.

The lower curves in Fig. 2 represent the intensity dependence of the SRS-A (curve *d*) and SRS-C (curve *c*) instabilities as determined from backscattering spectra such as those shown in Fig. 1. The limited sensitivity of the spectrographic measurements did not permit the observation of the $2\omega_p$ -instability reemission. Contrary to expectation, the onset of the SRS-C instability at approximately 500 nm occurs at almost the same intensity as the SRS-A instability, a point to be discussed later. A most significant aspect of all the curves shown in Fig. 2 is the saturation of the fractional scattered light energy from the $2\omega_p$ and SRS instabilities. Including the measured angular distribution of the backscattered light we find that typically no more than 10^{-6} of the incident light is scattered into the 700-nm components of the SRS or $2\omega_p$ -instability reemission. At present we are not aware of any existing applicable theory to predict this level of saturation. No comparable quantitative measurements are as yet available for the SRS-C instability. We also note that the SRS and $2\omega_p$ -instability signals were not measurably dependent on the irradiation spot size in these experiments.

The spectral distribution of the SRS-C instability near the threshold showed a peak around 520 nm. This wavelength was shorter than expected since the calculated gain maximum lies around $\omega_0/2$. SRS-C spectra were calculated by Williams, Bingham, and Short,⁷ following earlier work by Liu,⁸ including refraction and Landau damping. Reasonable agreement between the intensity dependence of the observed spectra and these calculations was obtained if the spectral dependence of both the SRS-C gain and the optical noise were included, together with an appropriate density profile. The optical noise was calculated for a 1-keV blackbody spectrum⁹ corrected for opacity. The lack of SRS-C signal between 610 and 700 nm requires a steepened density profile between $0.2n_c$ and $0.25n_c$. Such steepening, due to the ponderomotive forces generated by the intense

plasma wave fields, was found in plasma simulations by Langdon, Lasinksi, and Kruer,¹⁰ and was observed in CO₂-laser-produced plasmas by Baldis, Samson, and Corkum⁵ and in microwave plasmas by Mizuno *et al.*¹¹

The threshold for the convective Raman instability was not taken directly from Table I of Ref. 8, but was evaluated from the Rosenbluth gain formula¹² without approximating the wave vectors of the product waves by the pump wave vector. This threshold varies by a factor of about 2 over the range of wavelengths of interest and typical values are given below for a convective growth of a factor of 50 in intensity:

$$I_{2\omega_p} \approx 5 \times 10^{15} \frac{T_{\text{keV}}}{L_{\text{SRS-A}} \lambda_0}, \quad (1)$$

$$I_{\text{SRS-A}} \approx 5 \times 10^{17} \frac{1}{L_{\text{SRS-A}}^{4/3} \lambda_0^{2/3}}, \quad (2)$$

$$I_{\text{SRS-C}} \approx 2 \times 10^{17} \frac{1}{L_{\text{SRS-C}} \lambda_0}, \quad (3)$$

where $L_{\text{SRS-A}}$ is the density scale length near $n_c/4$, while $L_{\text{SRS-C}}$ is the density scale length below $n_c/4$ (L and λ_0 in micrometers, I in watts per square centimeter). $I_{\text{SRS-C}}$ is the intensity required for a convective gain of $50\times$, our best estimate of the instrumental detection threshold. For comparison of SRS-A and SRS-C thresholds we divide Eq. (3) by (2) to give

$$\frac{I_{\text{SRS-C}}}{I_{\text{SRS-A}}} \approx 0.4 \lambda_0^{-1/3} \frac{L_{\text{SRS-A}}^{4/3}}{L_{\text{SRS-C}}}. \quad (4)$$

The observations shown in Fig. 2 indicate the thresholds for the $2\omega_p$ and SRS-A instabilities to be 4×10^{13} and 4×10^{14} W/cm², respectively. These intensities are average values; however, the instabilities will grow from the peak intensities within the focal region, which are estimated to be 4 times larger. Thus, with peak intensities and a temperature⁹ of $T_e = 1$ keV, Eqs. (1) and (2) yield scale lengths at $n_c/4$ ($L_{\text{SRS-A}}$) between 100 and 140 μm . Two-dimensional hydrodynamic-code calculations¹³ predict considerably shorter scale lengths of 50 to 70 μm . In addition, using $L_{\text{SRS-A}} = 140$ μm and the experimentally observed ratio $I_{\text{SRS-A}}/I_{\text{SRS-C}} \approx 1$ we calculate from Eq. (4) $L_{\text{SRS-C}} \approx 400$ μm . The instability data and existing theory thus appear to require scale lengths twice as long as hydrodynamic model predictions at $n_c/4$ and even longer ones (5 to 8 times longer) at lower densities.

Filamentation in the plasma can be proposed as

an attractive explanation for the effective intensities and for the larger scale lengths inside the plasma. In many of the experiments, however, we observe a strong directionality in the light emitted at 700 nm from targets oriented at a significant angle to the incident laser beam. This suggests that for these experiments the plasma gradient was normal to the target and not significantly perturbed. Thus, filamentation may not explain all the observations.

We propose here an alternative model based on the fact that the instabilities at $n_c/4$ have typical growth regions of length l , such that $l \approx X_{\text{Debye}} \times (6\pi k_0 L)^{1/2} \ll L_{\text{SRS-A}}$, i.e., l is approximately a few microns. We postulate local regions (much smaller than the typical scale lengths) where the density gradients are shallower than implied by the overall scale length, i.e., $L_{\text{SRS-A}} > L_{\text{hydro}} \gg l$. Such density modulation could easily arise from density fluctuations produced near n_c which then propagate down the gradient through the region at $n_c/4$.

Once the absolute instabilities (SRS-A and/or $2\omega_p$) near $n_c/4$ have developed, steepening of the density gradient at $n_c/4$ may occur as discussed earlier. This process entails a plateau with a long scale length below $n_c/4$.^{5,11} Computer simulations¹⁰ indicate that this process leads to relaxation oscillations of the instabilities as well as the density profile near $n_c/4$. Thus the density step originating near $n_c/4$, along with the plateau below it, typically propagates down the gradient. This traveling plateau is then ideally suited for the growth of the SRS-C instability in the region below $n_c/4$.

Relaxation oscillations of the profile steepening near $n_c/4$ and the ensuing traveling density steps could well explain the apparent contradictions between the theoretical threshold predictions for the two Raman thresholds and the experimental observations of Fig. 2. While pulsing of the Raman scattered light and time-varying spectral distributions are consequences of this model, the complex spatial intensity distributions may easily mask the expected temporal signature.

In summary, we have observed clear evidence for the threshold behavior of the $2\omega_p$, SRS-A, and the SRS-C instabilities. The SRS-C instability is seen to occur over a density range of $0.2n_c$ to $0.05n_c$. Density steepening at $n_c/4$ can be inferred from the spectra. All measurements show saturation of these instabilities. Fractional back-scattering energies of 10^{-6} of the incident light are typical for the SRS-A instability and the $2\omega_p$,

instability reemission.

We gratefully acknowledge the invaluable technical support of R. Boni and B. Flaherty. We would like to thank R. Bingham and T. W. Johnston for many helpful and illuminating discussions. This work was partially supported by the U. S. Department of Energy Inertial Fusion Project under Contract No. DE-AC08-80DP40124 and by the Laser Fusion Feasibility Project at the Laboratory for Laser Energetics.

^(a)Also at Department of Mechanical Engineering, College of Engineering and Applied Science, University of Rochester, Rochester, N.Y. 14623.

¹R. E. Kidder, Nucl. Fusion **21**, 151 (1981).

²K. G. Estabrook, W. L. Kruer, and B. F. Lasinski, Phys. Rev. Lett. **45**, 1399 (1980); W. L. Kruer, K. Estabrook, B. Lasinski, and A. B. Langdon, Phys. Fluids **23**, 1326 (1980); N. A. Ebrahim, H. A. Baldis, C. Joshi, and R. Benesh, Phys. Rev. Lett. **45**, 1179 (1980).

³D. W. Phillion, Lawrence Livermore Laboratory Reports No. UCRL-84148, 1980, and No. UCRL-84854, 1980 (unpublished); K. Yamada and Y. Kato, in Institute of Laser Engineering, Osaka University, Japan, Report No. ILE-APR-79, 1980 (unpublished), p. 31.

⁴H. C. Pant, K. Eidmann, P. Sachsenmaier, and R. Sigel, Opt. Commun. **16**, 396 (1976); A. A. Offenberger, A. Ng, L. Pitt, and M. R. Cervenak, Phys. Rev. A **18**, 746 (1978); J. L. Bobin, M. Decroisette, B. Meyer, and Y. Vittel, Phys. Rev. Lett. **30**, 594 (1973); C. Garban, E. Fabre, C. Stenz, C. Popovics, J. Virmont, and F. Amiranoff, J. Phys. (Paris), Lett. **39**, L165 (1978); A. I. Avrov, V. Yu. Bychenkov, O. N. Krokhin, V. V. Pustovalov, A. A. Rupasov, V. P. Silin, G. V. Sklizkov, V. T. Tikhonchuk, and A. S. Shikanov, Zh. Eksp. Teor. Fiz. **72**, 970 (1977) [Sov. Phys. JETP **45**, 507 (1977)].

⁵H. A. Baldis, J. C. Samson, and P. B. Corkum, Phys. Rev. Lett. **41**, 1719 (1978).

⁶W. Seka, J. M. Soures, S. D. Jacobs, L. D. Lund, and R. S. Craxton, IEEE J. Quantum Electron. **17**, 1689 (1981).

⁷E. A. Williams, R. Bingham, and R. W. Short, Bull. Am. Phys. Soc. **26**, 863 (1981), paper No. 1U21.

⁸C. S. Liu, in *Advances in Plasma Physics*, edited by A. Simon and W. B. Thompson (Wiley, New York, 1976), Vol. 6, p. 121.

⁹B. Yaakobi, T. Boehly, P. Bourke, Y. Conturie, R. S. Craxton, J. Delettrez, J. M. Forsyth, R. D. Frankel, L. M. Goldman, R. L. McCrory, M. C. Richardson, W. Seka, D. Shvarts, and J. M. Soures, Opt. Commun. **39**, 175 (1981).

¹⁰A. B. Langdon, B. F. Lasinski, and W. L. Kruer, Phys. Rev. Lett. **43**, 133 (1979).

¹¹K. Mizuno, D. A. Rasmussen, J. S. DeGroot, W. Woo, and B. Till, Bull. Am. Phys. Soc. **26**, 861 (1981), paper No. 1U.

¹²M. N. Rosenbluth, Phys. Rev. Lett. **29**, 565 (1972).

¹³R. S. Craxton, private communication.